Numerical study on a hybrid mooring system with clump weights and buoys

*Zhiming Yuan [a], Atilla Incecik [a], Chunyan Ji [b]

[a] *Department of Naval Architecture, Ocean & Marine Engineering, University of Strathclyde, Glasgow, UK*

[b] *School of Naval Architecture and Ocean Engineering, Jiangsu University of Science and Technology, Zhenjiang 212003, China*

Abstract: A new hybrid mooring system based on the traditional taut mooring lines was proposed in the present study. A series of clump weights were attached to the lower end of each mooring line to form a catenary shape. Some buoys were connected to the upper ends of the lines to reduce the top tension on each mooring line. In order to verify the advantages of this new hybrid system, we investigated the motion responses of a semi-submersible platform moored by the proposed hybrid mooring system. The top tension on the lines was also calculated by using the time domain method. Comparing the results from the taut mooring system, it can be found that the tension on the lines could be reduced by using the present hybrid mooring system, while the motion responses were hardly influenced. Furthermore, a catenary shape was formed at the lower end of each mooring line, which could reduce the requirement of the anti-uplift capacity of the anchors. We also carried out the parametric study to investigate the optimal position and volume of the buoys. The discussions were highlighted on the influence of the water depth.

Key words: coupled analysis; time domain; hybrid mooring system; clump weights; buoys

1 Introduction

Deep-water floating systems are normally composed of three main components: the floating vessel, the mooring system (the mooring lines and the anchors) and the marine risers, all of which are subjected to the environmental loads. As a critical component, the mooring system guarantees the safety of the working condition of the vessel. For the water depths of up to 1000m, the most common mooring system is the catenary mooring system, which consists of a group of lines combined of chain and wire rope. For exploration and production in water depth beyond 1000m, the weight of the mooring line starts to become a limiting factor in the design of the floating system, and then the taut leg mooring system comes forth, which adopts synthetic polymeric ropes as the main section of the lines. In additional to these two popular mooring systems, a hybrid mooring system with buoys and catenary lines has been proposed these years.

There are mainly three aspects which can estimate the performance of a mooring system. The first one is the motion responses of the vessel. A smaller movement of the vessel will bring a better working condition for the floating structures. The second one is the tension on the mooring lines. It is obvious that a smaller tension is preferable in the design. But these two aspects are always incompatible. A smaller movement of the vessel can only be achieved when the mooring lines provide enough restoring forces, which requires a larger tension. The third one is the requirement for the anchor's holding capacity. The piles or suction anchor are required to resist significant vertical loads when there is a vertical component force at the anchor points, which will greatly increase the cost.

*Corresponding author at: Dep. of Naval Architecture, Ocean & Marine Engineering, University of Strathclyde. Henry Dyer Building, G4 0LZ, Glasgow, UK.
Tel: + 44 (0)141 548 2288. Fax: +44 (0)141 552 2879.
E-mail address: zhiming.yuan@strath.ac.uk

As for the catenary mooring system, the catenary chains or wires rely heavily on their own weight to provide restoring forces. As a result, it will not only increase the production costs, but also bring an increase to the top tension of the lines and enlarge the vertical loads on the vessel when the line is lifted from the sea bottom (Johanning, et al., 2007). This growth in vertical load can be important as it effectively decreases the vessel's useful payload. The restoring forces provided by catenary chain are not adequate to keep a small platform offset. However, the main advantage is that the anchors are only subjected to the horizontal force component since the lower end of the mooring line is resting on the seabed. As for the taut mooring system, the synthetic polymeric ropes can provide large restoring forces through their axial stiffness, which can reduce mean- and low-frequency platform offsets and improve the drilling condition. Meanwhile, the synthetic fibre lines are considerably light, very flexible and can absorb imposed dynamic motions through extension without causing an excessive dynamic tension. But the disadvantage is that the anchors need to handle a very large vertical.

The idea and application of the clump weights on the offshore mooring lines can be found in some previous publications. Finn (1976) proposed a new deep water offshore platform which was called 'the guyed tower', and the platform was held upright by multiple guy lines. Each line has three main portions: (1) A catenary from the fairlead connection at the tower to the clump weight; (2) a clump weight that is relatively massive compared with the cable; and (3) a line and an anchor pile to anchor the line. The clump weight rests almost entirely on the sea bottom during relatively small tower response. However, during the extreme sea state, the clump weights lift off the bottom to form part of an extended catenary from anchor pile to the tower. Morrison and Asce (1983) carried out the analysis for the dynamic properties of the guyed tower mooring lines. However, these researches are limited to the water depth up to 1500ft. Some other component mooring lines with additional sinkers and buoys are proposed recently. Smith and MacFarlane (2001) used catenary equations to solve a three component mooring made up of two lines, connected at a point buoy or sinker where water depth and fairlead tension were given. Vicente et al. (2011) investigated different mooring configurations with slack chain mooring lines of a floating point absorber with or without additional sinkers or floaters. It was found that the different arrangement of the buoys and weights would bring significant differences in terms of average and maximum tensions on the mooring cables. Hong and Kim (2004) carried out an experimental study for a compliant mooring system keeping a floating OWC device. The compliant buoy mooring system consists of four mooring systems, each of which has a buoy connected to horizontal and vertical mooring lines. However, this wave energy device was damaged by mooring line failure during a severe storm. This study has been made to clarify the mechanism of mooring line failure for future improvements in mooring line design.

Based on the guyed tower mooring lines, Ji et al. (2011) proposed a mooring system integrating catenary with taut mooring for deep water platform. In their study, some clump weights were applied to the lower end of the taut lines at fixed intervals, which could form a catenary end, tangent to the seabed. In that way, the anchor points were only subjected to the horizontal forces. They carried out the simulation for a semi-submersible. The results showed that the vessel's offsets and the line's tensions could be greatly reduced when the new mooring system was used. Besides, a catenary shape was formed at the lower end of the line, which lowered the requirement of the anti-uplift capacity of the anchors. It is also demonstrated by Yuan et al. (2011) that this combined mooring system was applicable for a wide range of water depth. But, as pointed by the author, the maximum tension of the new mooring system turned out to be a little larger when the water depth exceeds 1000m.

In this paper, a new hybrid mooring system with the clump weights and buoys will be proposed. It is based on the combined mooring system proposed by Ji et al. (2011). In the present work, some

improvements are made by attaching some buoys to the previous mooring lines. In this way, the top tension on the lines could be reduced. Meanwhile, this new hybrid system is expected to keep the merits of the previous one since the clump weights are retained.

2 Description of the new mooring system

The design of the present hybrid mooring lines is based on the traditional taut mooring lines. It can be seen from Fig. 1 that the mooring lines are connected to the floating structures and go in a fairly straight line to the bottom. This is only possible with light lines, therefore modern polyester lines are needed to achieve this. These lines have a large axial resistance and good fatigue properties. When the platform drifts horizontally with wind or current, the lines stretch and this sets up an opposing force. The lines usually come in at a 30 to 45 degree angle on the seabed where they meet the anchor, which is loaded vertically. Therefore, the suction piles must be used for deep water taut mooring lines to resist the vertical forces. Suction piles can be used in sand, clay and mud soils, but not gravel, as water can flow through the ground during installation, making suction difficult. And also suction piles are usually not allowed to be applied in reefs for the environmental protection. Furthermore, the installation and maintenance of the suction piles is very expensive.

In order to reduce the vertical component of the mooring force at the lower end of the mooring line, a series of clump weights are attached at the lower end of each line, which is shown in Fig. 2. And a couple of these mooring lines with clump weights can constitute a hybrid system, which can be called hybrid mooring system with weights (HMSW). It can be seen from Fig. 2 that the weights are attached to the lines at uniform intervals and the sizes of these weights decrease gradually from the sea bottom upwards. Therefore, the lower end of each line is expected to behavior as a catenary if the weights are arranged properly. When the lines are subjected to the maximum tension, it should be designed to fulfill the following condition: the clump weight (m_1 in Fig. 6) next to the anchor point should never be lifted off from the sea floor. Thus, it can be guaranteed that there is no vertical force at the lower end of the mooring line. When the tension decreases, the weights will be supported by the sea floor, thereby lowering the tension at the fairlead. However, in the numerical simulation (Ji et al., 2011), the tensions could be increased by the gravity of the weights. In order to lower the tension on the line, a buoy is attached to each mooring line, shown in Fig. 3. A couple of mooring lines with weights and buoys constitute a new hybrid system, which can be called hybrid mooring system with weights and buoys (HMSWB). The buoyancy of these buoys will counteract some of the gravity, and as a result, the tension on each mooring line can be reduced. The angle between the water line and the mooring line could also be reduced consequently. Thus, the horizontal restoring force provided by the line can be increased while the restoring forces in vertical direction will be reduced. Based on the same principle as the HMSW, the proper arrangement of the weights in HMSWB should also guarantee a horizontal alignment of the mooring line near the sea bed.

In engineering practice, the weights can be made from different materials with various shapes. The typical weights should be steel cubes, which are connected to the mooring chain by shackles. Each mooring line can be assembled onshore or on the board. Tugboats are in charge of towing the lines to the designated points. The buoys are widely used in deep water risers, and the installation technology could be similar. Compared to the suction piles, the manufacturing costs of the weights and buoys could be much lower. The difficulties involved in the installation of the new mooring system are quite different from the taut mooring system. The former rests with the towage of the lines to the designated points, while the latter involves in a suction (relative to seabed water pressure), which is applied within the pile and forces the pile to embed itself, leaving the top flush with the seabed. The scope of

application of the new hybrid mooring lines can be expanded to a wide range of seabed conditions, including sand, clay and mud soils, but also gravel and reefs. Besides, the new mooring lines are easy to recycle.

3 Formulations

The motion equation of the platform is combined with the mooring lines in the time domain as follows:

$$\left[M+\mu_{\infty}\right]\ddot{x}+\int_{0}^{\infty}R(t-\tau)\dot{x}d\tau+Cx=F^{fk}+F^{d}+F^{sd}+F^{w}+F^{c}+F^{m} \tag{1}$$

In the left hand side of Eq. (1), M is the structure mass, μ is the infinite added mass, $R(t-\tau)$ is the retardation function, C is the hydrostatic restoring coefficients. The added mass and radiation damping can be obtained by solving boundary value problem (BVP) and the retardation function can be obtained by inverse cosine Fourier transform of radiation damping. In the right hand side of Eq. (1), F^{fk} is the Froude-Krylov force, F^{d} is the diffraction force, F^{sd} is the second-order wave load, F^{w} is the wind load, F^{c} is the current load, F^{m} is transmitted force from the mooring line. The Froude-Krylov force and diffraction force can be obtained by solving boundary value problem (BVP) in frequency domain with the Fourier transformation. The second-order wave load is calculated by far field integration method in frequency domain with the Fourier transformation. Only horizontal second-order wave forces are calculated in the present study. The wave load is caused by average wind velocity and fluctuating wind velocity. It can be expressed by

$$F^{w}=C_{w}A_{w}v^{2} \tag{2}$$

where C_w is the wind force coefficient; A_w is projected area; v is the wind velocity. The time history of fluctuating wind velocity can be calculated by wind spectrum with Fourier transformation. In the present study, only horizontal wind loads (surge, sway and yaw) are calculated.

All body current forces are computed using the current velocity at the surface (z = 0). Traditionally, the viscous surge and sway force and yaw moment have been calculated based on current coefficients and the instantaneous magnitude of the translational relative velocity between the vessel and the fluid. The current drag forces are then expressed by (SIMO, 2009):

$$F^{c}(\alpha,t)=C_{1}(\alpha)\,|u|+C_{2}(\alpha)\,|u|^{2} \tag{3}$$

$$|u|^{2}=(v_{1}-\dot{x}_{1})^{2}+(v_{2}-\dot{x}_{2})^{2} \tag{4}$$

$$\alpha=\arctan\frac{v_{2}-\dot{x}_{2}}{v_{1}-\dot{x}_{1}} \tag{5}$$

where C_1 and C_2 are the linear and quadratic current force coefficients respectively; u is the relative velocity between low-frequency body velocity and current velocity; α is the relative angle between direction of low-frequency body velocity and current velocity; v_1 and v_2 are the longitudinal and transverse components of current velocity respectively; $\dot{x}_1$ and $\dot{x}_2$ are the surge and sway velocity respectively.

The present hybrid mooring lines are composed of four components: chain, polyester line, clump weights and buoys. Since the chain and polyester line are slender structures, the wave forces on these slender lines are calculated by using Morison's equation. The inertia and drag forces are usually computed separately for directions normal and tangential to the line, since the hydrodynamic coefficients in the two directions are different in general. The drag force per unit length is calculated as:

$$F^D = \frac{1}{2}\rho\pi D C_{dt} v_t |v_t| + \frac{1}{2}\rho D C_{dn} v_n^2 \tag{6}$$

where ρ is water density; D is the diameter of the line; C_{dt} is the nondimensional quadratic tangential drag force; C_{dn} is the nondimensional quadratic normal drag force; v_t and v_n are the tangential and normal flow velocity respectively. The inertia force per unit length is likewise calculated as:

$$F^I = \frac{1}{4}\rho\pi D^2 C_{mt}\dot{v}_t + \frac{1}{4}\rho\pi D^2 C_{mn}\dot{v}_n \tag{7}$$

where C_{mt} is the nondimensional quadratic tangential inertia force; C_{mn} is the nondimensional quadratic normal inertia force; $\dot{v}_t$ and $\dot{v}_n$ are the tangential and normal flow acceleration respectively.

The clump weights and buoys are treated as special elements with different mechanical properties. The loads on these elements are determined by their mass, volume and hydrodynamic coefficients. The drag forces acting on a buoy (or clump weight) are calculated according to the following formulae (DeepC, 2010):

$$F_x^D = \frac{1}{2}\rho B_x C_{dx} v_x |v_x| \tag{8}$$

$$F_y^D = \frac{1}{2}\rho B_y C_{dy} v_y |v_y| \tag{9}$$

$$F_z^D = \frac{1}{2}\rho B_z C_{dz} v_z |v_z| \tag{10}$$

where B_x, B_y and B_z are the projected area for flow in x, y and z direction individually; C_{dx}, C_{dy} and C_{dz} are the corresponding nondimensional drag coefficients; v_x, v_y and v_z are the flow velocity in x, y and z direction. The inertia forces acting on a buoy (or clump weight) are likewise calculated as:

$$F_x^I = \rho V C_{ax}\dot{v}_x \tag{11}$$

$$F_y^I = \rho V C_{ay}\dot{v}_y \tag{12}$$

$$F_z^I = \rho V C_{az}\dot{v}_z \tag{13}$$

where V is the volume of the clump weights (or buoys); C_{ax}, C_{ay} and C_{az} are the nondimensional inertia coefficients in x, y and z direction; $\dot{v}_x$, $\dot{v}_y$ and $\dot{v}_z$ are the corresponding flow acceleration in x, y and z direction.

4 Numerical study

4.1 Description of the platform

A typical semi-submersible (as shown in Fig. 4) in Gulf of Mexico is simulated to investigate the effectiveness of the proposed hybrid mooring system in different water depths. The horizontal *x-y* plane of the model is set on the base line with its origin placed on the center of the body, and z-axis is positive upward. The main particulars of the platform are summarized in Table 1. For the loading condition of the analysis, the 100-year extreme hurricane condition at GoM is used, which is one of the severest in the world. The summary of the environmental condition for this study is shown in Table 2. In the time domain analysis, the simulation duration of time is 600*s* with the time step of 0.2*s*. The ramp duration is 10s. Newmark integration procedure is applied with its integration operator β=0.25 and γ=0.5. The viscous roll damping fixed at 1500000 *kNs/m*.

4.2 Description of the mooring lines

The semi-submersible platform is moored by three different mooring systems: taut mooring system (TMS), hybrid mooring system with weights (HMSW) and hybrid mooring system with weights and buoys (HMSWB). The latter two systems can be classified as the hybrid mooring system (HMS). The only difference between TMS and HMS should be the weights and buoys as shown in Fig. 1-Fig. 3. Each mooring system is composed of 12 hybrid mooring lines, which is shown in Fig. 5. Table 3 gives the details of each mooring line. To compensate for the pretension from the risers and mooring lines, a vertical force of magnitude 2233*kN* pointing upwards is specified at CG of the platform.

As for the hybrid mooring system, five weights are attached at the lower end of each mooring line with a uniform spacing of 20 *m* (Fig. 6). The size of the weights decreases from the bottom upwards, where m_1=20 *t*, m_2=15 *t*, m_3=10 *t*, m_4=5 *t*, m_5=2 *t*. The buoys on each mooring line are designed to be sphere, attached 152 m away from the fairleads. The mass of the buoy is 2 *t*. The volume is 18m^3, and C_d=0.5, C_a=0.1.

4.3 Motion responses of the platform

The time history of sway, heave and roll motions of the platform moored by TMS, HMSW and HMSWB is shown in Fig. 7-Fig. 9. Table 4 gives the statistical variability of the standard deviations, the maximum and mean values of the motion responses. It can be found that the standard deviations of the sway response can be slightly reduced by using HMS (HMSW and HMSWB). The clump weights modify the configuration of the mooring lines. The static equilibrium position will be changed consequently. That is the reason for the large discrepancies of the maximum and mean values between TMS and HMS. For heave and roll motions, the difference of standard deviations between TMS and HMS is not evident. But, it can be observed that in heave motion, the mean value is slightly increased by using HMSW. This is because the clump weights will enlarge the top tension of the lines (as shown in Fig. 13) and the draft of the platform will be increased accordingly. But HMSWB can reduce the mean value of heave motion, since the top tension of the lines can be reduced by the attached buoys. By using fast Fourier Transform (FFT), the motion spectra of the platform can be obtained and plotted in Fig. 10-Fig. 12. The shapes of the spectral are similar and the difference of peak values is very small. The sway, heave and roll motions are dominated by wave frequency (WF) responses. Low frequency (LF) responses can also be observed in sway and roll motions, but it is not significant.

4.4 Tension on the mooring lines

We find that the static tension of Line 10 is the largest of all. Therefore, Line 10 is selected in this paper to investigate the tension results. Fig. 13 is the static tension of Line 10. It can be observed that the static tension keeps a downward trend as the lines extend to the sea bed and the element next to the fairlead is subjected to the largest tension. Comparing with TMS, HMSW could significantly increase the static tension on the mooring lines. But for the system with attached buoys (HMSWB), a very large reduction can be observed at the length ranging from 0 *m* to 152 *m* (the buoy is attached at 152 m away from the fairlead). After a sharp increase around 152 *m*, the static tension of HMSWB exceeds that of TMS and interposes between HMSW and TMS. It can also be found that the static tension changes slowly at the length ranging from 150 *m* to 1750*m*. This is because the material of the lines at this range is the polyester, which is much lighter than the chain segment at the lower and upper ends of the lines. At the lower end of the line, the last few elements keep a constant tension, which indicates these elements are resting entirely on the sea bed.

Fig. 14 shows the dynamic top tension on Line 10. Table 4 gives the statistical variability of the standard deviations, the maximum and mean values of the tension. It can be found that the standard deviations of the dynamic tension can be reduced by HMS. The clump weights behavior like a buffer, which can reduce the fluctuations of the tension. The buffering effect will be reduced by the attached buoys. It is the reason why the standard deviation of HMSWB is smaller than that of HMSW. But the buoys will reduce the mean and maximum values of the top dynamic tension. Fig. 15 is the tension spectrum results. The shapes of the three spectral are similar, while a very large discrepancy can be observed around the peak values. Consistent with the time history results, TMS has the largest peak value, followed by HMSWB and HMSW sequentially. It can also be observed that the wave frequency tension takes the dominate part.

4.5 Catenary end

The configuration of the lines is determined by the altitude value at each node. The position of each clump weight can be represented by its corresponding node. By linking all the nodes on the mooring lines, we can obtain the time series of the line shape. Fig. 16 (a) shows the catenary shapes of three different mooring systems at the moment when Line 10 is subjected to the maximum tension. It can be observed that the catenary shape has been achieved for both HMSW and HMSWB, while the shape of TML is almost a straight line. In order to investigate the difference between HMSW and HMSWB, we enlarge the plot for the last two nodes, which is shown in Fig. 16 (b). The two nodes at 1856 *m* and 1876 *m* of the line correspond to the position of m_2 and m_1 respectively, and 1896m is anchor point. As for HMSW, there is a slight lift height of m_1, which indicates the lines are not entirely tangent to the sea bed. But m_1 is resting on the sea bed entirely for HMSWB. It can be concluded that the buoys can some bring positive effects to form the catenary end. However, the buoys will bring more complexities, difficulties and costs to deepwater installation.

4.6 The effect of the buoys

The arrangement of the clump weights was discussed by Ji et al. (2011). This study will discuss the effect of the buoys. Line 10 is selected to investigate the line tension.

(1) The effect of the volume of the buoys

The volume of the buoys will influence the motions of the platform and the tension on the lines. In this paper, we make the optimal study over a wide range of the volumes (V=7m^3, 12m^3, 17m^3, 22m^3, 27m^3, 32m^3). The other parameters are kept unchanged.

The displacement in Fig. 17 indicates the offset ($D=\sqrt{x^2+y^2+z^2}$, x, y and z are the motion responses in surge, sway and heave direction) of CG. It can be observed that the displacement changes slowly as the buoy's volume increases from 7 m^3 to 22 m^3. But a sharp increase of displacement can be observed at the volume ranging from 22 m^3 to 32 m^3. To the contrary, the maximum tension on the lines keeps a downward trend (as shown in Fig. 18). It drops rapidly as the volume of the buoy increases from 7 m^3 to 22 m^3. The slope becomes very mild as the volume exceeds 22 m^3. Table 6 shows the effect of the volume on the hoisting height of m_1 and m_2 when the line is subjected to the maximum tension. As the volume varies from 12 m^3 to 22 m^3, the hoisting height of m_1 is 0, which indicates that m_1 is entirely resting on the sea bed. While in the other cases, there is a slight elevation of m_1. The hoisting height of m_2 experiences a decrease until the buoy volume increases to 17 m^3, and then the trend reverses. It can be concluded that the optimal volume should locate among 7 m^3 to 22 m^3 in the present study.

(2) The effect of the buoy position

In order to explore the effect of the buoy's position on the floating system, we make the parametric study over a range of distances (d=30 m, 60 m, 90 m, 120 m, 152 m; where d is the distance between the fairlead and the buoy). The volume of the buoys is fixed at 18 m^3. Meanwhile, all the other parameters keep unchanged.

The displacement in Table 7 indicates that there is only a very slight decrease of the displacement as the distance increases from 30 m to 152 m. But the static tension on the lines will be greatly influenced by the distance, as shown in Fig. 19. As the distance increases, the maximum static tension can be reduced accordingly. The maximum static tension can be found at the node corresponding to the buoys as the distance is smaller than 90 m. When the distance is greater than 90 m, the static tension at the fairlead becomes the largest one. An optimal design should guarantee that the distribution of the tension on the line is as equivalent as possible. Based on this principle, the distance in the present case study should be greater than 90 m. Consistent with the static tension results, the maximum dynamic tension also keep a downward trend as the as the distance increases from 30 m to 152 m, which can be observed from Fig. 20. Table 8 gives the hoisting height of m_1 and m_2 at different distance. We find m_1 is resting on the sea bed for all the distances we adopted in the present case study. However, the hoisting height of m_2 keeps a downward trend as the distance increases from 30 m to 152 m.

4.7 The effect of the water depths

In order to explore the application range of the proposed hybrid system, we make the comparison over a range of water depths (h=500 m, 750 m, 1000 m, 1500 m, 2000 m, 3000 m; where h is the water depth). All the parameters keep unchanged except the water depth and the line length shown in Table 9.

(1) Displacement of the platform

The statistical variability of the displacement is shown in Table 10 and Fig. 21. Overall, the trend of the displacement is upward as the water depth increases from 500 m to 3000 m. It can be found that the mean values of the displacement can be reduced by using the present HMS. But the difference between

HMSW and HMSWB is very small. The difference of the standard deviations is not evident between these three mooring systems.

(2) Tension on the lines

From Fig. 22 (a), it can be seen that the tension on the lines keeps a downward trend for all the three types of mooring system as the water depth increases from 500 *m* to 3000 *m*. It can be illustrated that the fluctuation of the line tension tends to be mild in deep water. It is also observed that the standard deviations of the tension of the hybrid mooring system (HMS, including both HMSW and HMSWB) is smaller than that of TMS, especially when the water depth is small. The standard deviation of HMSWB is slightly larger than that of HMSW due to the influence from the buoys.

The mean tension on the lines keeps an upward trend, as shown in Fig. 22 (b). Compared with TMS, the mean tension of HMSW tends to be larger due to the gravity of the weights. However, when the buoys are used, the mean tension of HMSWB can be even smaller than that of TMS. The buoyancy pointing upwards from the buoys can lower the tension on the upper ends of the mooring lines, which can also be observed from Fig. 13.

The comparison results of the maximum tension in Fig. 22 (c) are quite similar to the mean tension results at the water depth ranging from 1000 *m* to 3000 *m*. At 500 *m* water depth, the maximum tension of TMS tends to be the largest of all. It drops rapidly from 2140 *kN* to 1750 *kN* when the water depth increases from 500 *m* to 1000 *m*. But the changes of maximum tension of HMS are not significant at the water depth ranging from 500 m to 1000 m.

(3) Catenary end

Fig. 23 shows the catenary ends at different water depths. It can be found that at all water depths, a catenary shape can be formed by using the new hybrid mooring system. But, as it extends to the deep water, the lower ends are more likely to form a catenary shape.

5 Summary and conclusion

A new hybrid mooring system with clump weights and buoys was proposed in this paper. The validation was carried out based on the time domian coupled analysis method. Through the comparison between HMS and TMS, the following conclusions can be drawn:

1. The present hybrid mooring system could reduce the displacement of the platform. But the reduction is not evident.

2. The attached buoys could reduce the tension on the mooring lines. This is a significant improment for the mooring system since it provides a good approach to solve the contradiction between the vessel's motion and the line's tension.

3. The catenary end could be formed through an optimal arrangement of the weights and buoys. There was only horizontal component of the loads at the anchor point. As the water depth increses, the mooring lines were more likely to rest on the sea bed and form a catenary shape.

4. The volume and position of the buoys could bring a significant influence to the line's tension. But the influence on the vessel's motion and catenary end is not evident.

5. The present hybrid mooring system has a wide range of the application. At water depth ranging from 500 *m* to 3000 *m*, it provides a satisfied performance.

Overall, the numerical results indicate that the present hybrid mooring system with clump weights and buoys will bring improvement to the vessel's offsets and the line's tension. It can form a catenary shape at the lower end of the lines, which guarantees that there is only horizontal component of the loads at the anchor point. However, the buoys will bring more complexities, difficulties and costs to deepwater installation. Further replenishment will focus on the experimental study, which will be carried out in the future work.

6 Acknowledgements

This study was supported by the National Natural Science and Foundation of China (Grant No. 51379095).

7 References

DeepC, 2011. DeepC User Manual. Version 4.5-05.

Finn, L.D., 1976. A new deepwater offshore platform- the guyed tower. In: Offshore Technology Conference, Houston, Texas.

Hong, S.W., Kim, J. H., 2004. Experimental Study of a Compliant Mooring System for a Floating OWC Device, Proceeding of The Fourteenth International Offshore and Polar Engineering Conference, Toulon, France.

Ji, C.Y., Yuan, Z.M., Chen, M.L., 2011. Study on a new mooring system integrating catenary with taut mooring. China Ocean Engineering, 25(3), 427-440.

Johanning, L., Smith, G.H., Wolfram, J., 2007. Measurements of static and dynamic mooring line damping and their importance for floating WEC devices. Ocean Engineering, 34:14-15, 1918-1934.

MARINTEK, 2009. SIMO Theory Manual. Version 3.6.

Morrison, D.G., Asce, A.M., 1983. Guyed tower with dynamic mooring properties. Journal of Structural Engineering 109, 2578-2590.

Smith, R. J., MacFarlane, C. J., 2001. Statics of a three component mooring line. Ocean Engineering 28, pp.899–914.

Vicente, P.C., Falcão, A.F., Justino P. J., 2011. Slack-chain mooring configuration analysis of a floating wave energy converter. 26th International Workshop on Water Waves and Floating Bodies, Athens, Greece.

Yuan, Z.M., Ji, C.Y., Chen, M.L., Zhang, Y., 2011. Coupled analysis of floating structures with a new mooring system. 30th International Conference on Ocean, Offshore and Arctic Engineering, , Rotterdam, The Netherlands.

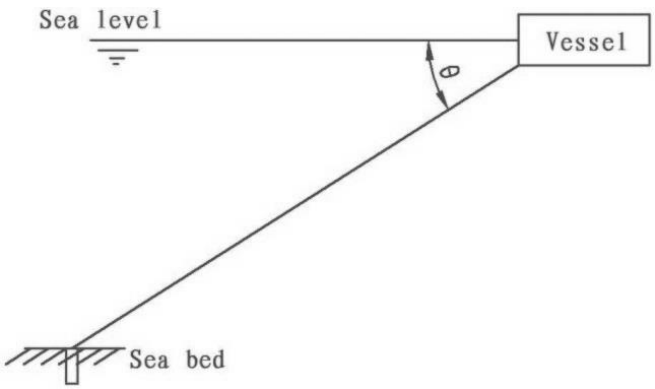

Fig. 1 Taut mooring line (TML)

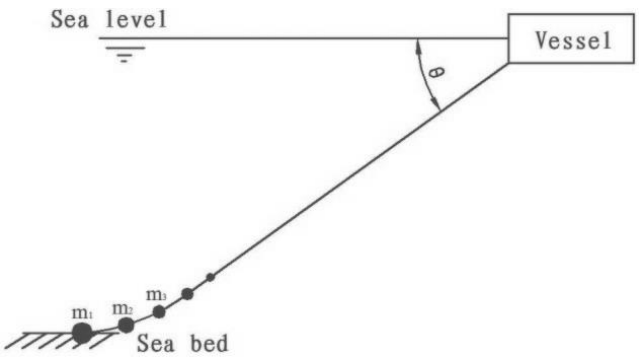

Fig. 2 Hybrid mooring line with clump weights (HMLW)

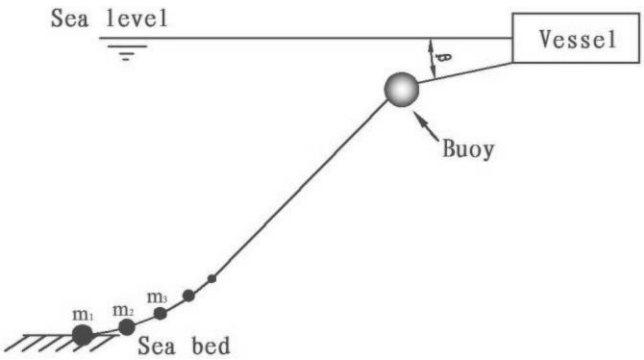

Fig. 3 Hybrid mooring line with clump weights and buoys (HMLWB)

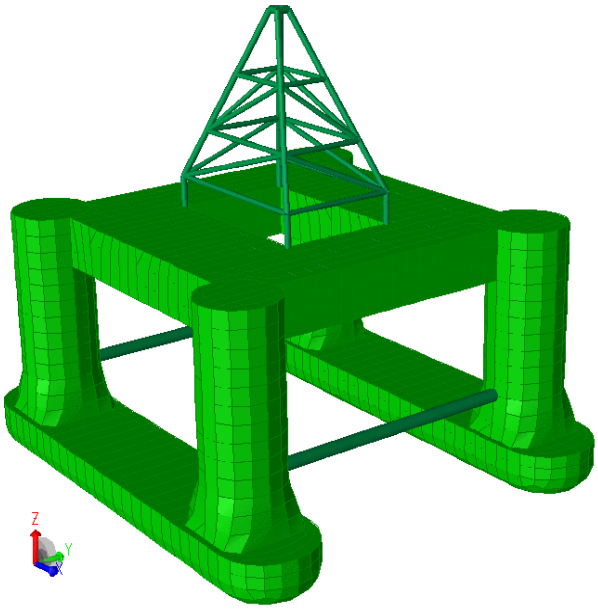

Fig. 4 Semi-submersible platform model

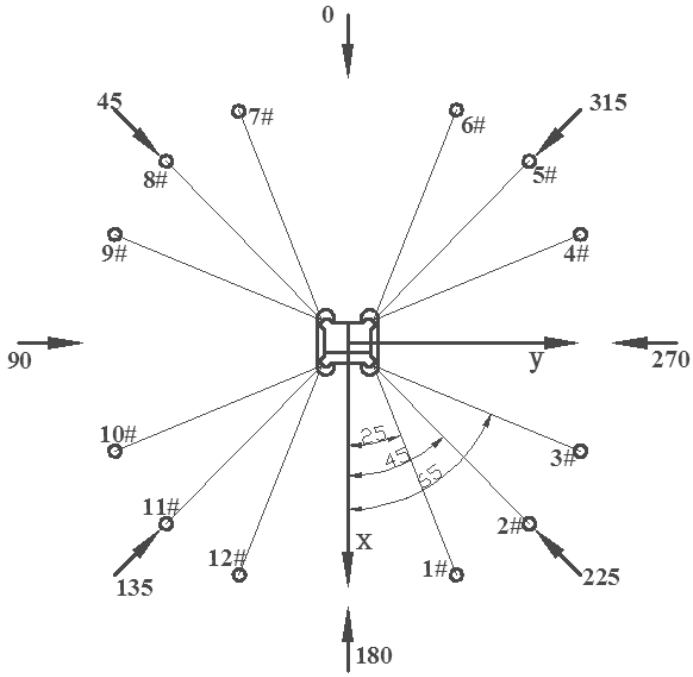

Fig. 5 The arrangement of the mooring lines

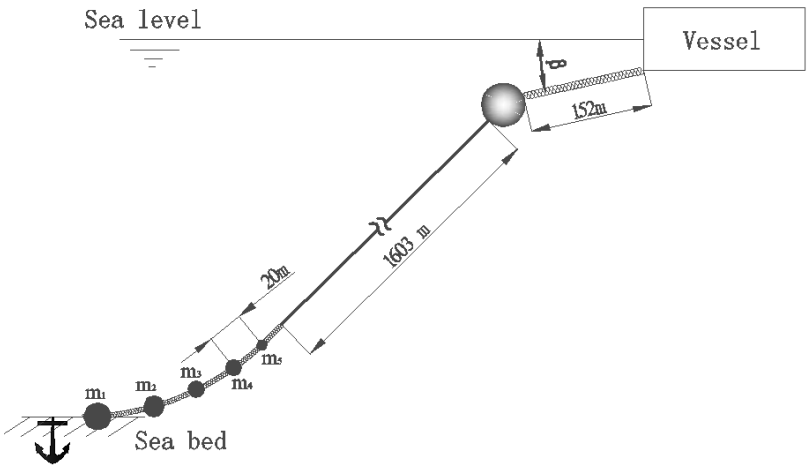

Fig. 6 Hybrid mooring lines

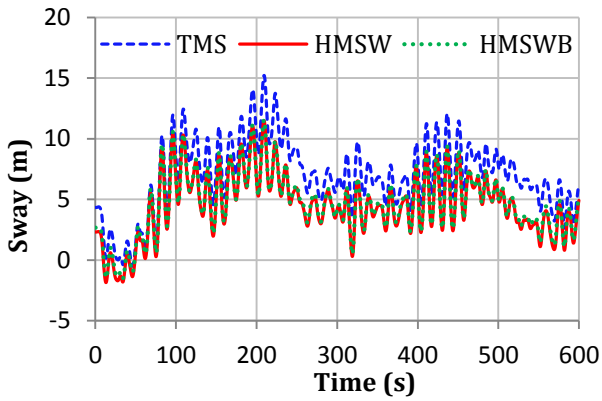

Fig. 7 Time history of sway

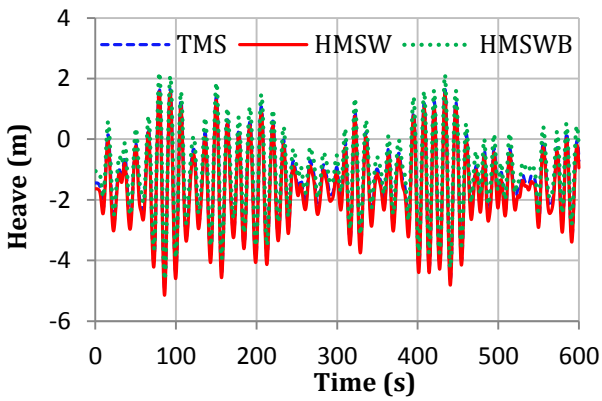

Fig. 8 Time history of heave

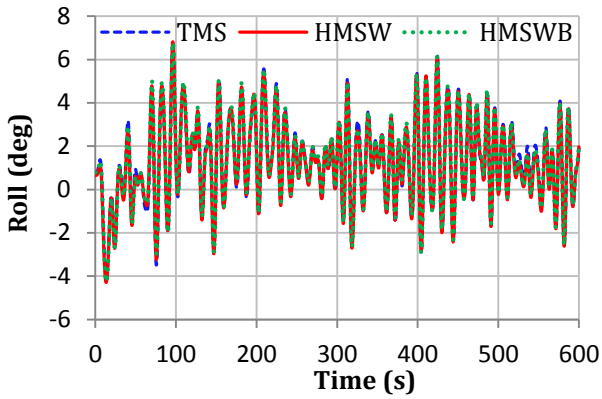

Fig. 9 Time history of roll

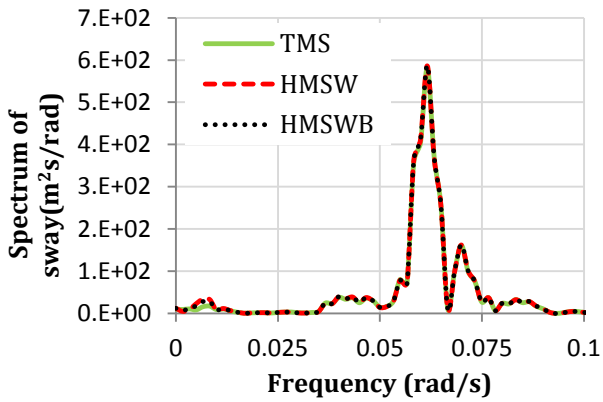

Fig. 10 Spectral density of sway

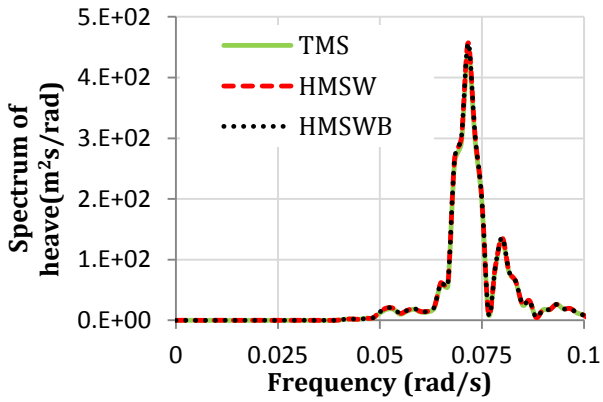

Fig. 11 Spectral density of heave

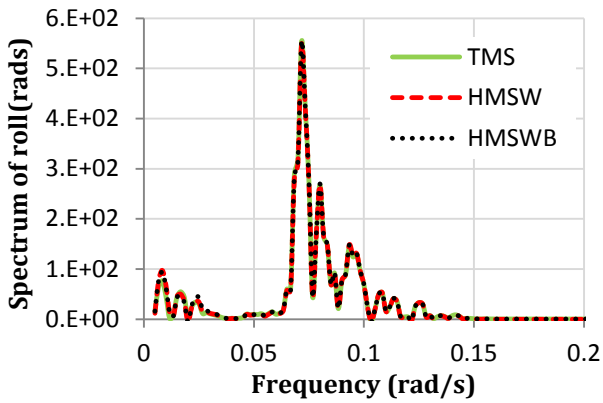

Fig. 12 Spectral density of roll

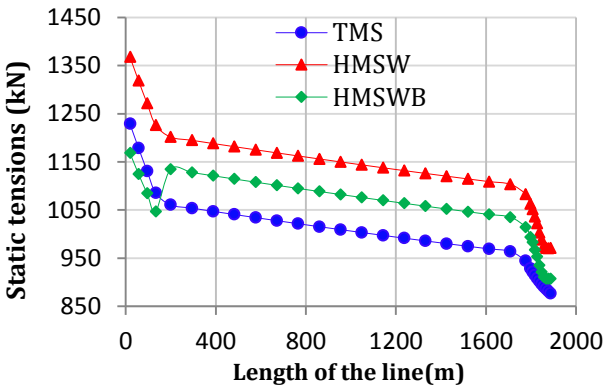

Fig. 13 Static tension

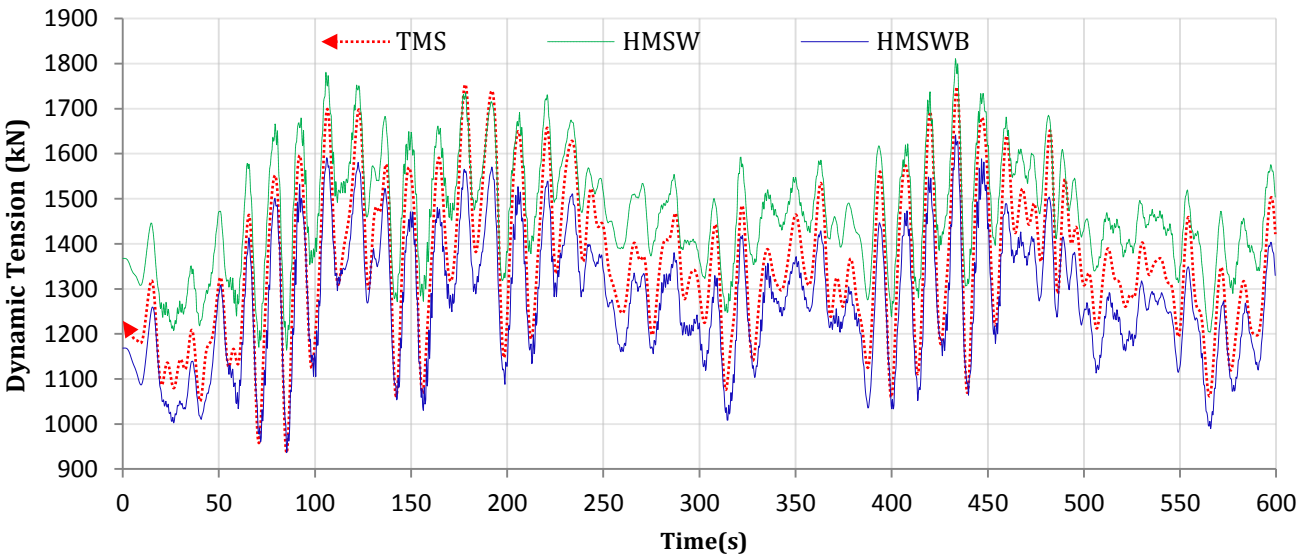

Fig. 14 Dynamic top tension

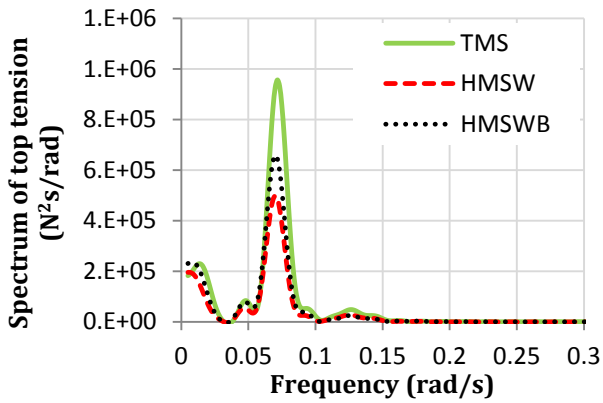

Fig. 15 Tension spectra

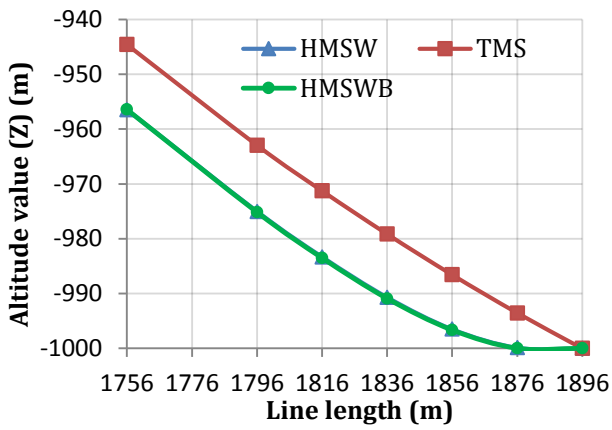

(a)

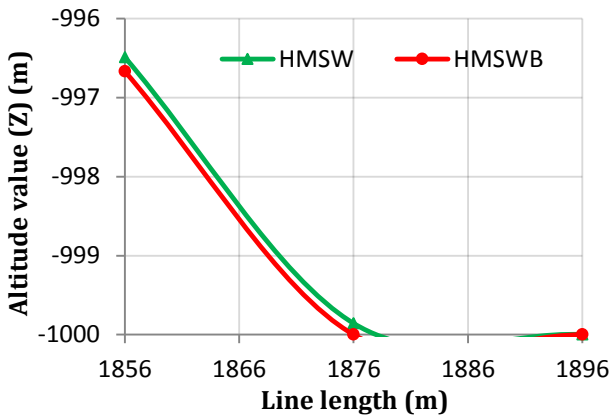

(b)

Fig. 16 Catenary end

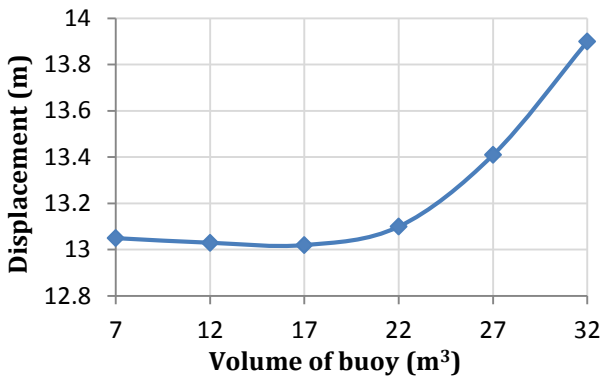

Fig. 17 The displacement of the platform

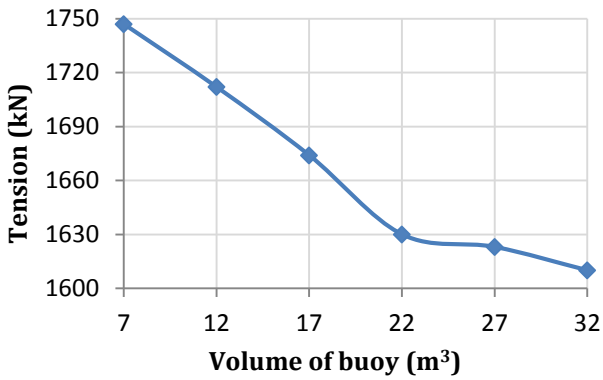

Fig. 18 Tension on the lines

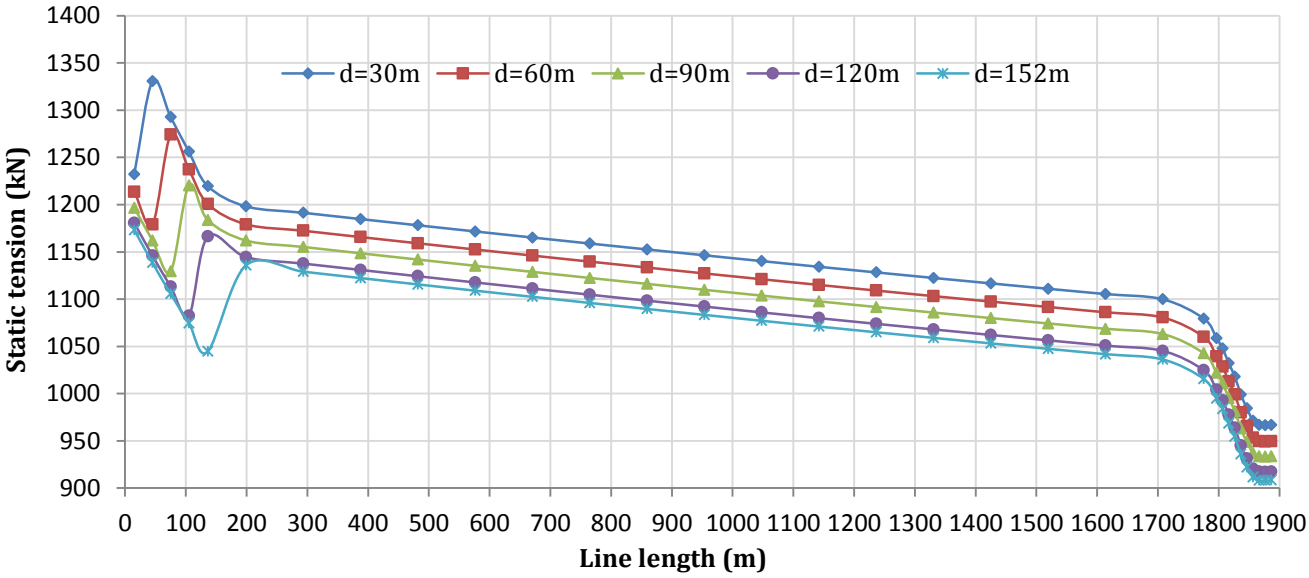

Fig. 19 Static tension at different distances

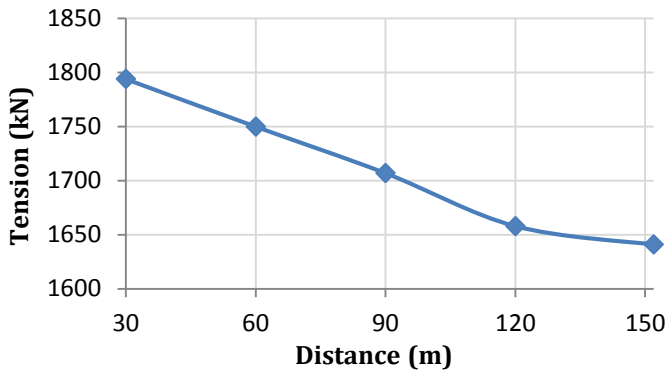

Fig. 20 The maximum dynamic tension of different distances

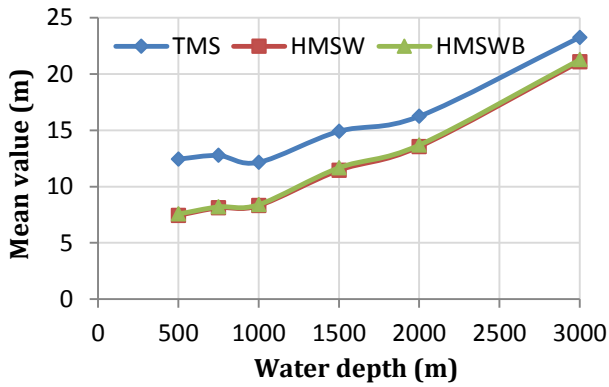

(a)

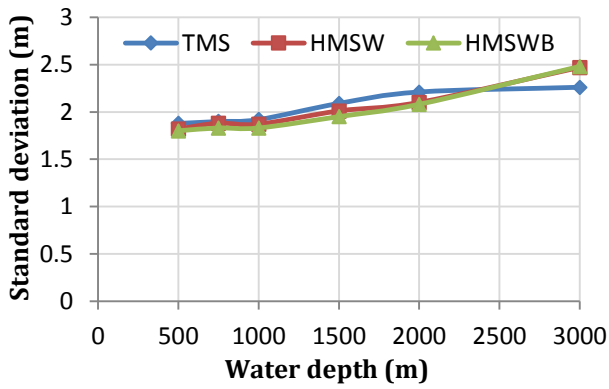

(b)

Fig. 21 The displacement at different water depths. (a) Mean values; (b) Standard deviations.

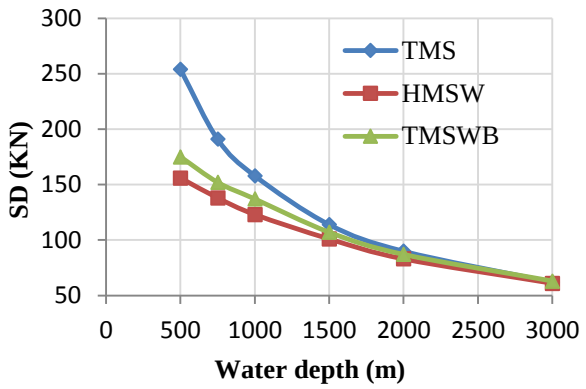

(a)

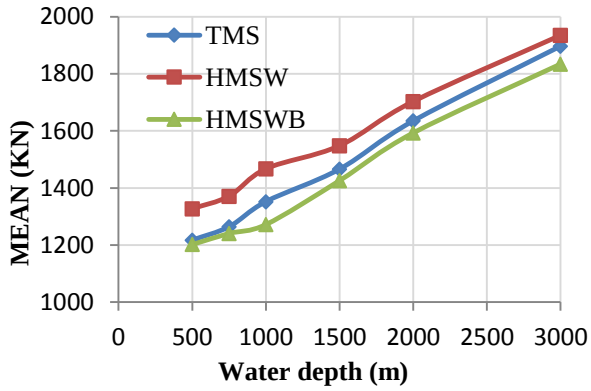

(b)

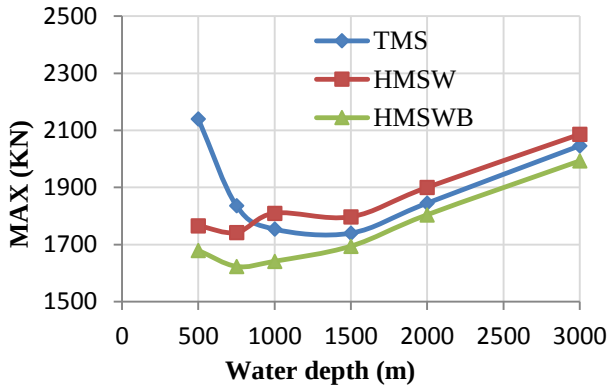

(c)

Fig. 22 Tension on the lines at different water depths. (a) Standard deviations; (b) Mean tension; (c) Maximum tension.

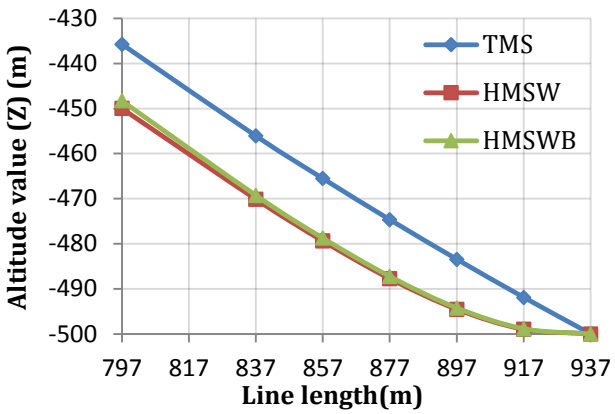
-430
-440
-450
-460
-470
-480
-490
-500
Altitude value (Z) (m)
797
817
837
857
877
897
917
937
Line length(m)
TMS
HMSW
HMSWB

(a)

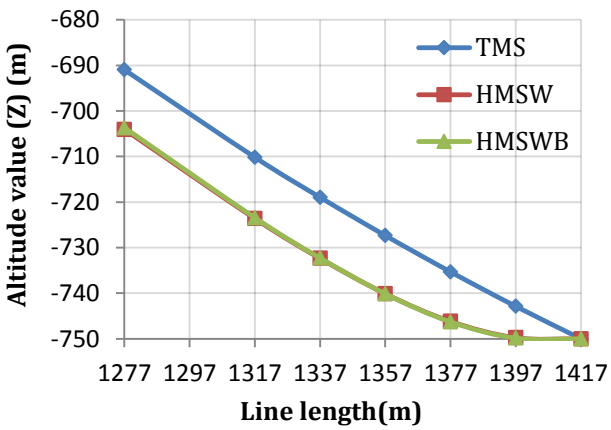
-680
-690
-700
-710
-720
-730
-740
-750
Altitude value (Z) (m)
1277
1297
1317
1337
1357
1377
1397
1417
Line length(m)
TMS
HMSW
HMSWB

(b)

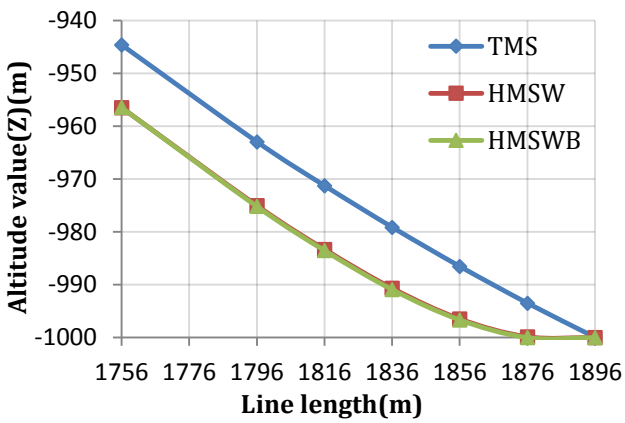
-940
-950
-960
-970
-980
-990
-1000
Altitude value(Z)(m)
1756
1776
1796
1816
1836
1856
1876
1896
Line length(m)
TMS
HMSW
HMSWB

(c)

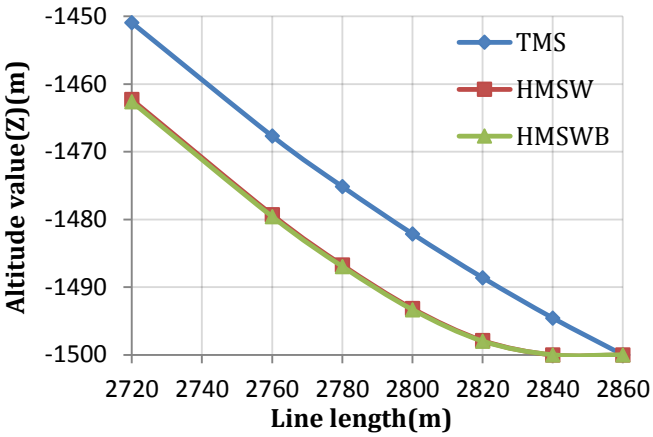

(d)

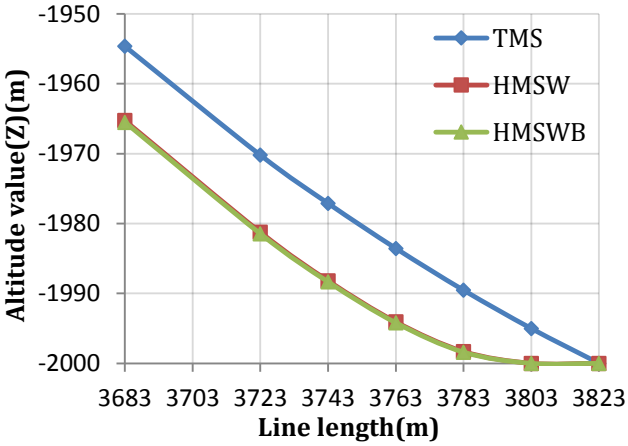

(e)

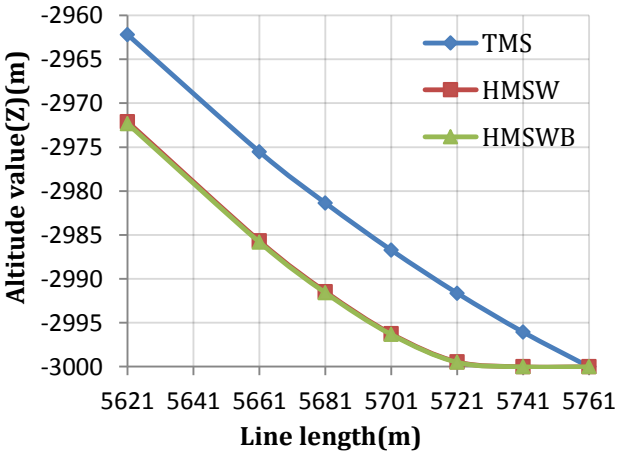

(f)

Fig. 23 The catenary ends at different water depths. (a) 500 m; (b) 750 m; (c) 1000 m; (d) 1500 m; (e) 2000 m; (f) 3000 m.

Table 1 Main particulars of the platform

Length (*m*)	80.6
Breadth of pontoon (*m*)	16
Height of pontoon (*m*)	7.5
Diameter of columns (*m*)	12.9
Spacing of columns (*m*) (centre to centre)	54.72
Displacement (m^3)	23548
Distance between pontoons (*m*)	1.17
Vertical position of CG (above BL) (*m*)	14.9
Longitudinal coordinate of CG (forward midship) (*m*)	0
Radius of inertia for pitch (*m*)	30
Coordinate of Fairlead 1 (*m*)	(33.6, 29.0, 0)
Coordinate of Fairlead 2 (*m*)	(31.9, 32.9, 0)
Coordinate of Fairlead 3 (*m*)	(29.0, 33.6, 0)

CG, centre of gravity; BL, base line

Table 2 Environmental loading condition

Wave	
Wave spectrum	JONSWAP
Significant wave height (*m*)	12.19
Peak period (*s*)	14
Direction (*deg*)	90
Wind	
Wind spectrum	API RP 2A-WSD
Velocity (*m/s*)	41.12
Direction (*deg*)	60
Current	
at free surface (0 *m*) (*m/s*)	1.0668
at 60.96 m (*m/s*)	1.0668
at 91.44 m (*m/s*)	0.0914
on the sea bottom (*m/s*)	0.0914
Direction (*deg*)	120

Table 3 Main particulars of the mooring lines

Segment	Length (*m*)	Diameter (*m*)	Wet Weight (*t/m*)	EA(*MN*)	C_{dn}/C_{dt}	C_{mn}/C_{mt}	MBL (*kN*)
Chain	152	0.098	0.192	802	2.45/0.65	2/0.5	8927
Polyester	1603	0.178	0.007	300	1.2/0.3	1.15/0.2	9786
Chain	141	0.098	0.192	802	2.45/0.65	2/0.5	8927

Table 4 Statistical variability of the motions

Motion	Statistical variability	TMS	HMSW	HMSWB
Sway(m)	MAX	15.21	11.48	11.57
	Mean	6.92	4.53	4.75
	SD	2.98	2.62	2.55
Heave(m)	MAX	-4.92	-5.15	-4.62
	Mean	-1.47	-1.64	-1.07
	SD	1.25	1.27	1.27
Roll(deg)	MAX	6.74	6.82	6.76
	Mean	1.36	1.28	1.37
	SD	1.86	1.88	1.89

MAX: maximum value; SD: standard deviations

Table 5 Statistical variability of tension (unit: *kN*)

	Mean	SD	Max
TMS	1355	158	1753
HMSW	1469	123	1810
HMSWB	1274	137	1641

Table 6 The hoisting height of m_1 and m_2

Volume (m^3)	Hoisting height of m_1 (m)	Hoisting height of m_2 (m)
7	0.02	3.34
12	0	3.31
17	0	3.3
22	0	3.33
27	0.01	3.46
32	0.02	3.81

Table 7 Displacement (unit: *m*)

d	30	60	90	120	152
Disp.	13.34	13.33	13.32	13.18	13.10

Table 8 The hoisting height of m_1 and m_2

Volume (m^3)	30	60	90	120	152
Hoisting height of m_1 (m)	0	0	0	0	0
Hoisting height of m_2 (m)	3.33	3.26	3.23	3.17	3.12

Table 9 The length of the mooring lines at different water depths (unit: *m*)

Water depth	500	750	1000	1500	2000	3000
Upper Chain	152	152	152	152	152	152
Polyester Line	644	1124	1603	2567	3530	5468
Lower Chain	141	141	141	141	141	141
Total Length	937	1417	1896	2860	3823	5761

Table 10 The displacement of the platform at different water depths (unit: *m*)

Water depth	TMS			HMSW			HMSWB		
	Mean	SD	Max	Mean	SD	Max	Mean	SD	Max
500	12.45	1.88	17.56	7.44	1.82	12.12	7.56	1.80	12.27
750	12.77	1.90	17.82	8.11	1.88	12.94	8.20	1.83	12.96
1000	12.16	1.92	17.22	8.30	1.87	13.17	8.39	1.83	13.10
1500	14.91	2.09	20.24	11.44	2.01	16.80	11.67	1.95	16.86
2000	16.24	2.21	21.79	13.54	2.10	18.99	13.69	2.08	19.07
3000	23.25	2.26	29.57	21.09	2.47	27.18	21.28	2.48	27.32

Table 11 Tension on the lines at different water depths

Water depth (*m*)	TMS			HMSW			HMSWB		
	Mean *(kN)*	SD *(kN)*	Max *(kN)*	Mean *(kN)*	SD *(kN)*	Max *(kN)*	Mean *(kN)*	SD *(kN)*	Max *(kN)*
500	1217	254	2140	1327	156	1766	1202	175	1679
750	1264	191	1836	1371	138	1742	1241	152	1623
1000	1352	158	1754	1467	123	1810	1272	137	1641
1500	1466	114	1740	1548	101	1797	1426	107	1694
2000	1635	90	1845	1703	83	1900	1593	87	1804
3000	1897	62	2046	1935	61	2086	1834	63	1993